IEEE Access
Multidisciplinary | Rapid Review | Open Access Journal

Received March 14, 2022, accepted April 13, 2022, date of publication April 25, 2022, date of current version May 2, 2022.

Digital Object Identifier 10.1109/ACCESS.2022.3170243

Enhanced Signal-Associated Noise in a φ-OTDR System

MALAK GALAL, SUNEETHA SEBASTIAN, AND LUC THÉVENAZ, (Fellow, IEEE)
École Polytechnique Fédérale de Lausanne, 1015 Lausanne, Switzerland

Corresponding authors: Malak Galal (malak.galal@epfl.ch) and Suneetha Sebastian (suneetha.sebastian@epfl.ch)

This work was supported in part by the Horizon 2020 Framework Program through the Marie Skłodowska-Curie Grant "ITNFINESSE" under Grant 722509, and in part by Innosuisse under Grant 579292.

ABSTRACT Owing to their high sensitivity with respect to external measurands, Rayleigh-based distributed optical fiber sensors (DOFS) find their way into applications in many industrial and academic sectors. To further transcend the limit of these sensors in terms of sensing range, low spatial resolution, speed and accuracy of the measurement, improving the signal-to-noise ratio (SNR) of the system plays a pivotal role. Out of the several existing techniques for enhancing the SNR, one such method, solely dedicated to the Rayleigh-based sensors, is through intrinsically increasing the backreflected signal of the fibers. The enhanced backreflected signal provided by such fibers, generally known as reflection-enhanced fibers (REF), is rigorously analyzed in the present work. It is inferred from the analysis that the enhanced signal is essentially accompanied by enhanced signal-dependent noises, which can adversely affect their performance. For instance, when a performance comparison is carried out between the REF and a standard single-mode fiber (SMF) under identical experimental conditions, due to their different intrinsic backreflected signal levels, the two fibers experience dissimilar noise regimes leading to an erroneous estimation of the performance of the former. This necessitates the optimization of the interrogation system and the experimental parameters while employing such fibers for specific sensing applications. Additionally, a distributed temperature measurement is presented by taking advantage of the enhanced SNR of a 100 m long REF exhibiting a sub-mK temperature uncertainty of 0.5 mK at metric spatial resolution yielding a sixfold improvement compared to the 3 mK uncertainty of an SMF.

INDEX TERMS Distributed optical fiber sensors, temperature sensors, Rayleigh scattering, enhanced reflection, signal-dependent noises, optical time-domain reflectometry.

I. INTRODUCTION

Distributed optical fiber sensors (DOFS) are at the core of numerous fields, especially the ones in which spatial temperature profile measurements are required to be performed for long lengths, for example like in applications that include structural health monitoring. In such fields, highly stable and accurate distributed temperature sensors are invariably required to anticipate any possible faults that could lead to hazardous damages. Indeed, vast research has been carried out in that regard with the goal of reaching the best performances of such sensors in terms of accuracy. The signal-to-noise ratio (SNR) of the back-scattered light of any DOFS plays a crucial role when it comes to sensing for long distances yet aiming at achieving highly reliable and fast measurements. The proven inverse relationship of the SNR and the measurement uncertainty in the case of Brillouin-based [1] as well as Rayleigh-based DOFS [2] oriented the highly demanding and purely fundamental research towards improving the SNR of the systems with the ultimate goal of reaching the highest measurement accuracy [3]–[5].

One of the most common techniques adopted to achieve SNR enhancement in Rayleigh-based sensors relies on the core manipulation of the sensing fiber, thereby inducing supplementary density fluctuations in the fiber core which in turn results in higher Rayleigh scattering. Therefore, several studies in the literature proposed different approaches to increase the scattering centers along the fiber, for instance with the use of nano-particle doping achieving a back-scatter enhancement of 36.5 dB, yet a round-trip loss of 25.5 dB/m [6], or using UV exposure reaching 50 dB of signal enhancement with a 0.15 dB/m induced loss [7], [8], along with others.

An inevitable repercussion of improving the Rayleigh back-scattering through the enhanced *isotropic* scattering by

The associate editor coordinating the review of this manuscript and approving it for publication was Sukhdev Roy.

inducing more scattering centers is the increased total loss in the fiber; ergo, only short distance sensing would be possible. For instance, let us assume a scenario in which a 30 dB enhancement in the backreflected signal is achieved at the expense of a fiber loss of around 0.2 dB/cm. In such case, the accordingly enhanced backreflected signal will result in a higher/equivalent back-scattered power only up to a distance of ∼74 cm when compared with a standard SMF (0.2 dB/km). Thus, considering the total cost of manipulated fibers along with the added fiber losses, the real essence of the higher SNR obtained by increasing the number of scattering centers is quite skeptical. However, such fibers can still find a panoply of applications which don't demand long range distributed sensing yet require high accurate measurements of the measurand, such as in biomass reactors, nuclear reactors, and others. Thus far, the lowest achieved temperature uncertainty is 0.85 mK using a 10 mm gauge and a loss of 0.08 dB/m [9].

As a consequence of the high loss induced by the scattering centers, the spotlight has been turned on the inscription of faint Bragg gratings along the sensing fiber to benefit from an enhanced *directional* backreflected signal with a fairly low fiber loss [10], [11]. In [12], [13], Westbrook *et al.* presented a reflection-enhanced fiber (REF) using a standard single-mode fiber (SMF) which has overlapped chirped Bragg gratings inscribed in its core. Accordingly, a ∼ 10 dB *directional* enhancement over a bandwidth of ∼ 12 nm from 1544 nm to 1556 nm was achieved, whereas the optical losses were measured to be below 0.7 dB/km [14]. Whilst such reflection-enhanced fibers are extensively employed in several experiments based on φ-OTDR [15], the effect of the experimental conditions on the performance of these fibers has not been examined so far and is yet to be discovered further. For instance, in our own previous work making use of such an REF [16], having a ∼10 dB back reflection enhancement, the observed temperature resolution enhancement is just three times even though the inverse relationship exists between the SNR and the uncertainty of the measurement [2]. This observed discrepancy in the inverse relationship between the SNR and the uncertainty of the measurement led us to thorough analysis of the signal from such backreflection-enhanced fiber. The work presented here is, therefore, utterly significant to the optical fiber sensing researchers who deal with such reflection-enhanced fibers for various distributed measurements.

In this paper, we analyze how the performance of such REF would be impacted by a highly-sensitive interrogation system like the commonly-utilized φ-OTDR. From our studies, we found out that the intrinsic backreflected signal enhancement of the REF makes the fiber essentially highly susceptible to the signal-dependent noises and environmental fluctuations in φ-OTDR systems. Consequently, we carefully analyzed the signal-dependent noises to maximize the benefit of the fiber's signal enhancement. To that effect, we yielded an improved measurement accuracy with a fairly low temperature uncertainty of 0.5 mK for a 1 m spatial resolution, as a pure consequence of the increased SNR, when compared with the SMF.

II. ABSOLUTE REFLECTIVITY OF THE FIBERS

The backreflection coefficient (α_{bs}) which is a measure of the back-scattering coefficient and the back-scatter re-capture fraction of the fibers under consideration, is measured using a standard incoherent OTDR setup. The REF used in our experiments is the *AcoustiSens* GS82628 fiber from OFS company [14]. It demonstrated a backreflection coefficient of ∼-64.1 dB/m which is roughly 8.7 dB higher than that of a standard SMF which has a value of ∼-72.8 dB/m. This 8.7 dB is considered as the absolute value of the optical backreflected intensity enhancement provided by the REF as illustrated in Fig. 1, when interrogated using an OTDR system.

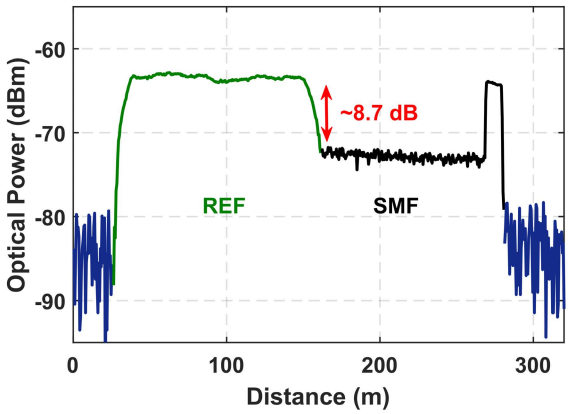

FIGURE 1. Backreflected signal from the REF and the SMF measured using an incoherent OTDR. Note: The blue traces before and after the fibers represent the noise floor. The spike before the noise floor is the reflection at the fiber end.

When compared with a typical incoherent OTDR, φ-OTDR is a highly sensitive interrogation technique for Rayleigh-based DOFS [17], which makes the measurements highly susceptible to environmental fluctuations. The intrinsic backreflected signal enhancement in the REF makes it even more prone to environmental fluctuations and other signal-dependent noises in the system. Hence, the mitigation of such signal-dependent noises is highly essential to fully exploit the signal enhancement provided by the REF into an effective SNR enhancement. In this context, we observed that conventional methods used to further improve the SNR of the system, for instance through trace time-averaging or straightforwardly by increasing the input optical power to the fiber (below the onset of nonlinear effects) would not necessarily yield the expected results. The investigation on this phenomenon is presented in great detail in the following section.

III. NOISES IN A φ-OTDRSYSTEM

A. THEORETICAL ANALYSIS

In the direct-detection φ-OTDR setup illustrated in Fig. 2, the possible noises in the system responsible for the variation

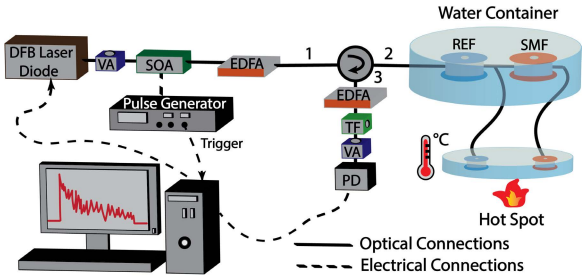

FIGURE 2. Experimental setup of a frequency-scanned φ-OTDR using direct detection.

of the photocurrent of the photo-detector are the thermal and the shot noises of the PD along with the signal-ASE beating noises originating from the pre-amplifier used before the PD. It ought to be remarked that the effect of the ASE-ASE beating noise is insignificant in our system due to the use of an optical filter after the optical amplifier, and is accordingly not considered in the overall system noise. As a result, the standard deviation of several consecutive time-domain traces, σ_n, which is a measure of the total detected noises in the PD can be expressed as [17], [18]:

$$\sigma_n = \sqrt{\sigma_{th}^2 + \sigma_{sh}^2 + \sigma_{signal-ASE}^2} \tag{1}$$

where σ_{th}^2, σ_{sh}^2, and $\sigma_{signal-ASE}^2$ are the variances of the thermal noise, shot noise, and signal-ASE beating noise, respectively. σ_{th} is independent of the optical power of the back-scattered light (P_{bs}) to the PD, whereas the σ_{sh} and σ_{ASE} are dependent on P_{bs} through a square-root relationship [18]. The SNR of the system which is estimated directly from the time-domain trace following an exponentially-decaying probability density function is given by:

$$\text{SNR} = \frac{\mu_{P_{bs}}}{\sigma_n} \tag{2}$$

Here, $\mu_{P_{bs}}$ is the mean of the backreflected signal and σ_n is the standard deviation of the electrical amplitude of the reflected optical signal along the fiber, for 20 consecutive measurements. It should be mentioned that the electrical amplitude of the signal is equivalent to the optical power through the conversion gain of the photo-detector. Besides, P_{bs} can be calculated theoretically from the equation given below:

$$P_{bs} = P_{in}\, \alpha_{bs}\, R_{sp} \exp(-2\alpha z) \tag{3}$$

where P_{in} is the input peak power to the fibers under consideration, α_{bs} is the backreflection coefficient, R_{sp} is the spatial resolution of the system and α is the attenuation coefficient of the fiber, and the factor 2 accounts for the round-trip distance traveled by the light to reach the receiver at the input of the fiber.

The impact of the variable attenuation utilized before the PD in the φ-OTDR setup (Fig. 2) should, of course, be taken into consideration when calculating the effective gain provided by the pre-amplifier [18]. In the present work, the average power to the PD is maintained well below saturation by means of a variable attenuator.

B. EXPERIMENTAL SECTION

The most commonly-used experimental setup of a direct-detection frequency-scanned φ-OTDR is implemented for the present study as shown in Fig. 2. It utilizes a distributed feedback (DFB) laser, at 1550 nm having a linewidth around 5 MHz, as the coherent probing light source followed by a high extinction ratio (ER) semiconductor optical amplifier (SOA) connected to a pulse-generator for the generation of optical pulses with a pulse width (τ) of 10 ns. An Erbium-doped fiber amplifier (EDFA) boosts the pulse power which is then reduced using a variable attenuator (VA) before the pulse enters the fibers to prevent the occurrence of nonlinear optical effects. The light pulse passes through the circulator, then enters into the fibers under test which are immersed in a water bath to reduce the influence of the environmental fluctuations. The pulses travel through the backreflection-enhanced fiber followed by a single-mode fiber, each of around 100 m long. The splice loss at the junction between the two fibers is negligibly small to ensure the same exact conditions for both fibers. It is worth noting that the order of the positioning of the two fibers as first or second will not cause the signal to reach the second fiber with lower intensity and therefore worse SNR conditions. This is mainly because of two reasons: firstly, the total attenuation coefficient of the kind of REF that we opted for in the present scenario is very negligible (when considering such a short fiber length), and secondly, the splice loss at the junction is ensured to be as small as possible, thereby guaranteeing that the two fibers are experiencing the same experimental and detection conditions. A 5 m long hot spot is chosen at the end of each fiber spool, and kept in a temperature-controlled water bath to perform the temperature measurement. To perform the frequency scan over a 13 GHz range with a step of 17 MHz, the injection current of the laser driver is remotely swept. The backreflected signal directed through port 3 of the circulator gets amplified again by means of a second EDFA, and enters a 1 nm optical tunable filter (TF) which minimizes the ASE-ASE beating noise generated by the EDFAs. The back-scattered light intensity from the fibers is received by a 1 GHz photo-detector (PD). The photocurrent generated in the PD is then acquired by a data acquisition card (DAQ) at a sampling rate of 500 MS/s.

C. EXPERIMENTAL ANALYSIS

To understand the influence of the different noises (mentioned in section III-A) on the SNR improvement of the system with respect to the backreflected signal, the input power to the fibers under consideration is varied. The evolution of the SNR as a function of the backreflected power (P_{bs}) from the two sets of fibers is illustrated in Fig. 3. It can be clearly seen that for a given input peak power (P_{in}) to the fibers and considering their lengths of 100 m each, the SNR of the REF is always higher than that of the SMF due to the intrinsic increase in the backreflection coefficient (α_{bs}) of the

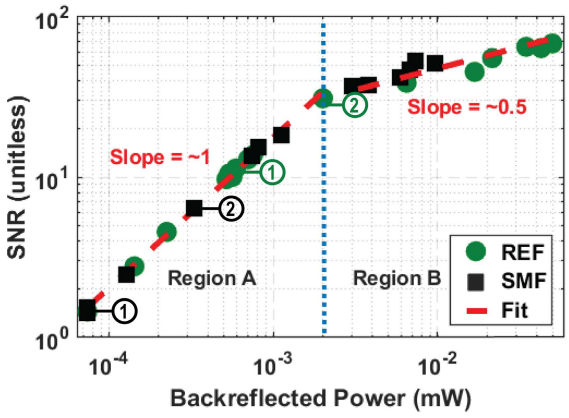

FIGURE 3. Log-log graph showing the SNR as a function of the backreflected power for both fibers. The encircled numbers mark SNR values at two different input peak powers for both fibers (black circles for SMF, green circles for REF). The same number corresponds to the same input power for the two fibers; (1) corresponds to an input power of ~18.9 dBm and (2) corresponds to ~25.4 dBm.

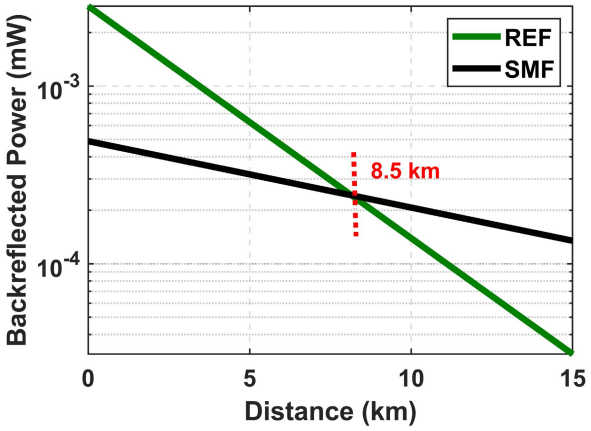

FIGURE 4. Semi-log graph showing the backreflected power as a function of the fiber length for both fibers calculated using Eq. 3 highlighting the contribution of the loss term.

former. Additionally, the evolution of the SNR with respect to the input power (or backreflected power) of the REF is very similar to that of the SMF, but at a noticeably faster rate. There are two distinct regimes of interest in terms of the SNR improvement shown in Fig. 3. In the first region (Region A in Fig. 3), the SNR of the system is improved linearly (slope of ~1 in the log-log graph of Fig. 3) with respect to the input/backreflected power to/from the fiber. This is mainly because σ_n in Eq. 2 is dominated by signal-independent noise, namely σ_{th}. In the second region (Region B), the SNR of the system is improved with a square-root dependency (slope of ~0.5 in the log-log graph of Fig. 3) with respect to the backreflected power. At these powers, σ_n is dominated by the signal-dependent noises. Under the given experimental conditions (such as 1 m spatial resolution and length of the fibers of 100 m each), a P_{bs} value of 0.002 mW (corresponding to an SNR of ~33.9 or 15.3 dB in the dB-scale) is the threshold below which the SNR of the fibers increases linearly with respect to the input peak power/backreflected power.

As mentioned in the earlier paragraph and as can be seen from Fig. 3, the SNR of the REF is always higher than that of the SMF irrespective of the kind of noises affecting the SNR. This implies that a better SNR is achieved with such backreflection-enhanced fibers as long as the contribution of the exponential term in Eq. 3 is lower than the enhanced backreflection coefficient (α_{bs}). In this particular kind of REF, having an α_{bs} of ~-64.1 dB/m and α of ~0.7 dB/km, a higher P_{bs} is observed up until a fiber distance of ~8.5 km (Fig. 4). Beyond this length, because of the increased loss in the REF, P_{bs} of the SMF will take over the performance of the former.

It is interesting to further analyze the consequences of this change of regime for different sensing configurations and thus to determine under what conditions the SNR could be impaired. In an optimized configuration for a sensor of given fiber length, the input peak pulse power to the fiber (P_{in}) is set at its maximum possible value, which is the critical power P_{crit} allowed below the onset of nonlinear effects in the fibers, mainly the effect of modulation instability [19]. Assuming a spatial resolution of 1 m and varying the sensing fiber length, the threshold value of P_{bs} (0.002 mW, under the present experimental conditions) is obtained when the total length of the REF is around 300 m. Since α_{bs} of the SMF is lower than that of the REF, this value is reached when the length is around 50 m. This implies that when using P_{crit} as the input power to the fibers under consideration, they will be in the thermal noise regime (Region A in Fig. 3) when the length of the fibers is greater than 300 m and 50 m for the REF and the SMF, respectively. For any length of the fibers that is shorter than these values, at the P_{crit}, the noise regime of the fibers can only be in Region B in Fig. 3. The noise regime in Region B is therefore predominant only for short sensing ranges and, regarding the negligible effect of attenuation over such short distances, is observed at all positions over this fiber length. As a corollary a change of spatial resolution will modify the critical length of the fiber proportionally (e.g. a 2 m spatial resolution will extend the limit lengths shown in Fig. 5 by a factor 2).

These numbers are critically related to the noise level of the optical amplifier and can certainly vary depending on the devices used in the experimental setup. However, the noise level is observed to stay in a given range in most commonly used amplifiers and the numbers presented here can be safely considered as a good representation of a general situation.

We further demonstrate a peculiar situation in which there is dissimilarity in the noise regimes between the REF and the SMF with the aid of Fig. 6 for a given input power. Fig. 6 (a) shows the Rayleigh back-scattered optical intensity time-domain traces and Fig. 6 (b) shows the standard deviation traces of several consecutive time-domain traces of the REF and the SMF for an input peak power of 25.4 dBm. It should be mentioned that the two sets of fibers are adjoined such

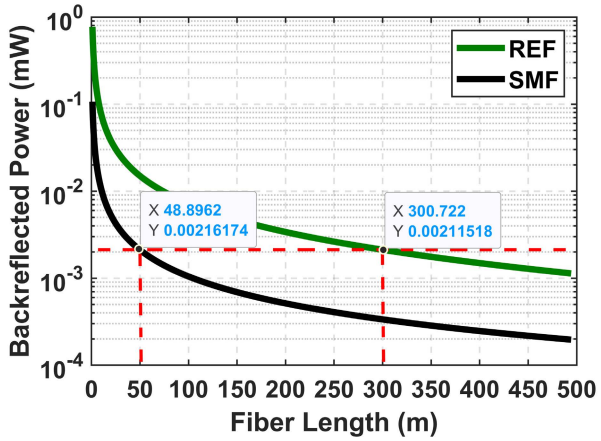

FIGURE 5. Semi-log graph showing the backreflected power as a function of distance for both fibers calculated using Eq. 3 where the input peak power is taken as P_{crit}.

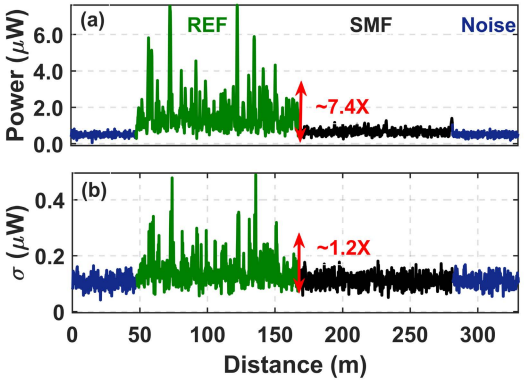

FIGURE 6. (a) Time-domain trace (optical power) along the distance of the fiber; (b) The standard deviation of 20 time-domain traces corresponding to input peak powers of around 25.4 dBm. Note: The blue traces before and after the fibers represent the noise floor.

that the signals received at the PD from the fibers experience the same experimental and detection conditions. Under these conditions, the signal enhancement provided by the REF (estimated from the mean of the time-domain trace) is nearly 7.4X (∼8.7 dB) higher than that of the SMF (Fig. 6 (a)). The REF/SMF standard deviation ratio is around 1.2X (Fig. 6 (b)), yielding an overall 7.9 dB higher SNR for the REF when compared to the SMF, instead of a full SNR increase of 8.7 dB higher. That is because at the used input peak power of 25.4 dBm, signal-dependent noises are more prominent in the case of the REF, whereas in the case of the SMF, the overall noise is limited by the thermal noise of the detector. This claim is evident from Fig. 6 (a) and (b), and can be further substantiated by Fig. 7 which shows the cross-correlation between the time-domain trace and the standard deviation trace of Fig 6. A clear correlation peak is observed for the REF, but as expected there is zero correlation for the SMF. This rather simple correlation technique between the time-domain trace and the standard deviation trace clearly points out whether the noises are signal-dependent or not.

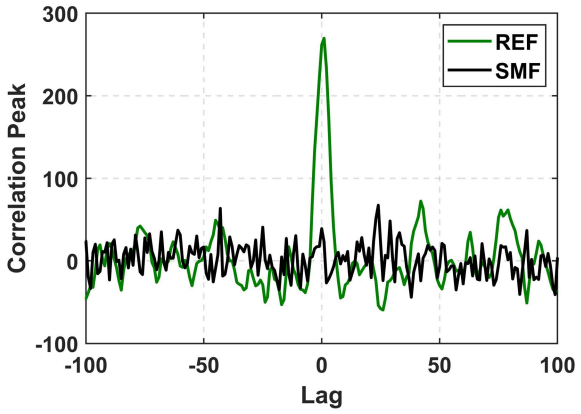

FIGURE 7. Cross-correlation between the time-domain traces and the standard deviation traces of Fig. 6.

As can be seen on Fig. 6 (b), the mean of the standard deviation of the SMF matches well with the mean of the noise floor of the system confirming that for the given input power to the fibers, the SMF is thermal noise limited, whereas the REF is not.

This is a crucial inference because the SNR improvement provided by the REF is not always exactly matching with the signal enhancement when put in comparison with the SMF at a given input power. For this difference in the SNR to be maintained between the REF and the SMF, both of them should share similar standard deviation of the measurement. Having different sets of noises in the two different fibers can lead to an erroneous estimation in the physical parameters like temperature uncertainty when a comparison is made. Hence, the present analysis of the enhanced signal from the REF highlights the need of regulation of the input power to such fibers and the optimization of the interrogation setup to yield the best performance.

We have also analyzed the SNR dependency on the number of time-averaged traces, and confirmed the square-root dependence (slope of 0.5 in a log-log graph) in the case of the SMF, but the dependence was slightly different for the REF (slope of 0.2 in a log-log graph). The range of averages between 1 and 2048 averages is applied to the traces, and already at 8 averages the difference in the slope is observed. This again implies a slower rate in the SNR increase for the REF. Since this result is quite surprising, we speculate that this discrepancy is possibly occurring because of other sources of noises that take place when the duration of the experiment is extended (e.g. signal distortions due to environmental fluctuations). We further confirm our speculations by nullifying this anomaly using a real-time data acquisition card (DAQ), thereby yielding a square-root dependence of the SNR with respect to the number of averages for both fibers.

To sum up, the management of the number of time-averaged traces (if no real-time DAQ is available) as well as the input power to such backreflection-enhanced fiber is vital to benefit from its full potential. It should

be considered that the higher intrinsic signal enhancement, like in the REF, is always accompanied by higher signal-dependent noises and any increment in the input power (even though well below the onset of the nonlinear effects) will not necessarily yield the expected SNR enhancement as explained earlier. Hence, addressing the signal-dependent noises is crucial to understand how to utilize the full potential of such fibers.

IV. DISTRIBUTED TEMPERATURE SENSING USING THE REF

Despite the fact that using such backreflection-enhanced fibers can be quite tedious due to the continuously interfering system noises, they can be really beneficial in DOFS, provided the experimental setup is fully optimized. One interesting characteristic offered by backreflection-enhanced fibers, as a pure consequence of the enhanced SNR, is a fairly better spectral shift quality as can be in Fig. 8. This quantity can be explained as the measure of the correlation strength between two data sets, when interrogated using a φ-OTDR setup. Commonly, when a frequency-scanned φ-OTDR system is employed, the correlation strength can be significantly improved (at a given SNR), and large correlation errors can be mitigated when the frequency scan range of the probe pulse is sufficiently large [20]. Yet, a large scan range requires a longer measurement time. However, if the SNR is high enough with the aid of a fiber like the REF, the scan range can be significantly reduced leading to much faster measurements.

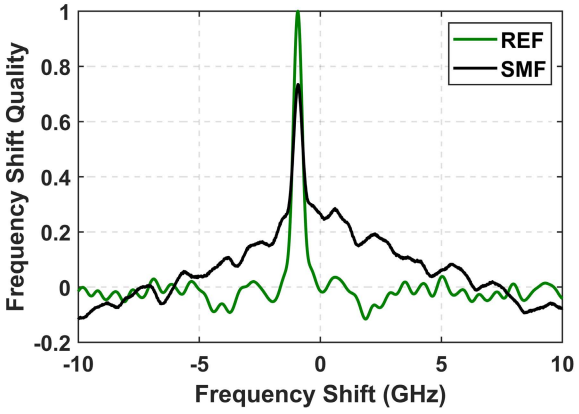

FIGURE 8. Local correlation as a function of the frequency shift at an arbitrary position in the two fibers.

Under the same amplification and detection conditions, and by taking utmost advantage of the qualities exhibited by the REF, a distributed temperature measurement with the REF and the SMF is performed with the setup shown in Fig. 2. In our own previous work [16], we observed an unexpected disparity in the temperature resolution improvement. The improvement in the temperature resolution was not following the inverse relationship with the increase in the SNR, when compared between the SMF and the REF. As mentioned in the previous section, for the given input power, the total noise of the REF was dominated by the signal-dependent noise (thereby higher σ_n), whereas for the SMF it was the signal-independent noise dominating. This apparently reduced the SNR difference between the two sets of fibers below the intrinsic value of 8.7 dB. Such an erroneous estimation can be made very commonly due to the lack of the awareness of the different noises playing the role for the same input power.

Thus, in the present case this is mitigated by controlling the experimental conditions. The input peak power launched into the fibers under test is 25.4 dBm and no averages were applied to the traces, so as to avoid any environmental fluctuation, such that a proper 8 dB difference between the two fibers is attained. Since the frequency shift uncertainty of the measurement, in a Rayleigh-based DOFS, is inversely proportional to the optical SNR of the signal, it is expected that the temperature uncertainty of the REF will be much lower than that of the SMF, for a given set of experimental conditions. The upper figure of Fig. 9 shows the frequency shift of the Rayleigh back-scattered intensity of the REF and SMF over a range of 10 K. The inset in the figure shows the frequency shift of the temperature measurement as a function of distance and highlights the position of the hot spot in the two fibers under consideration. The linear fit of

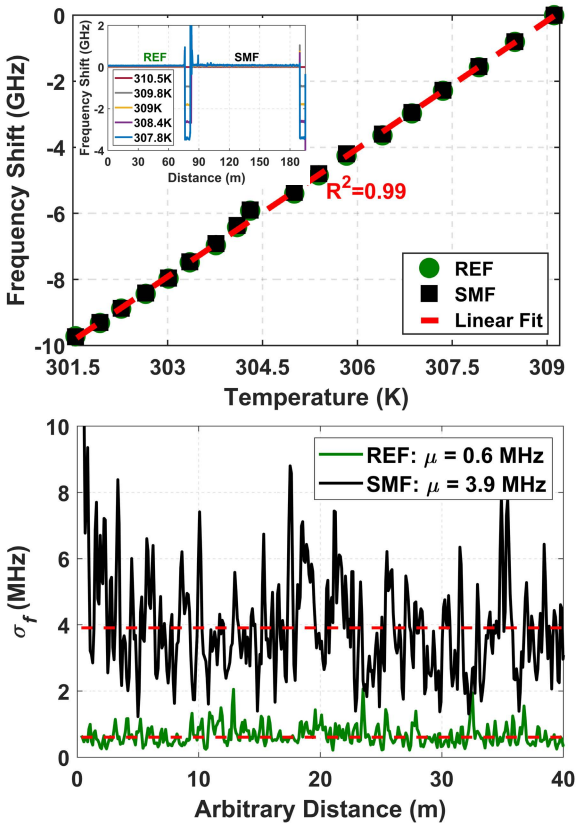

FIGURE 9. Upper figure: Frequency shift as a function of temperature; and the frequency shift versus the distance along the fiber (inset).; Lower figure: Experimental frequency uncertainty as a function of an arbitrary distance of 40 m in each fiber; theoretical values (red dashed line).

the plot yielded a correlation coefficient of 0.99, and the sensitivity obtained from the slope, for both REF and SMF, is 1.29 GHz/K. This implies that, despite the modifications of the fiber core due to the presence of continuous Bragg gratings throughout the REF, the thermo-optic coefficient of the original silica fiber is not altered, thereby showing the same temperature sensitivity as that of the SMF.

The frequency uncertainty (σ_f) of the temperature measurement calculated from the traces for an arbitrary fiber distance of 40 m (shown in the inset of the upper figure of Fig. 9) as well as the theoretical uncertainty calculated using the model presented in [2], [21] are illustrated in the lower figure of Fig. 9. As can be seen, for the REF, the mean value of the uncertainty is found to be 0.6 MHz, for a metric spatial resolution, which is nearly 6.5X lower than that of the SMF. This significantly low uncertainty value for the REF is a pure consequence of its ∼6.5X (∼8 dB) higher SNR, and this can be corroborated by our recently published work [2], in which we found out that, for a Rayleigh-based sensing system using a rectangular input pulse, σ_f is inversely-related to the SNR as given by the following equation:

$$\sigma_f = \frac{\sqrt{6}}{2\pi\,\tau\,M_o} \tag{4}$$

where τ is pulse width and M_o is the system SNR for optical power. The temperature uncertainty, σ_t, is in turn given as a function of σ_f as follows:

$$\sigma_t = \frac{\sigma_f}{S} \tag{5}$$

where S is the temperature sensitivity (1.29 GHz/K) of the fibers under test. Using Eq. (5), which provides a direct relation between σ_t and σ_f, the temperature uncertainty obtained when using the REF is as low as 0.5 mK, whereas that of the SMF is 3 mK which is the generally known value for standard single-mode fibers for metric spatial resolution.

V. CONCLUSION

In this paper, we present a thorough study on the use of a backreflection-enhanced fiber in a φ-OTDR system. The backreflection coefficient of this fiber (∼-64.1 dB/m) is found to be about 8.7 dB higher than that of a standard SMF. However, from our experiments, we realized that the experimental conditions of commonly-used highly sensitive systems (e.g. φ-OTDR) have a vital impact on the performance of such fibers due to the inevitable signal-dependent noises associated with the REF intrinsic signal enhancement. This necessitates the need for optimizing the experimental conditions when such fibers are interrogated. Hence, with careful handling of these noises, we were able to exploit the REF to maximum effect in a distributed temperature measurement reaching a sub-mK temperature uncertainty of 0.5 mK with metric spatial resolution, zero trace averaging and small scan range of the laser probe pulse.

(Malak Galal and Suneetha Sebastian contributed equally to this work.)

REFERENCES

[1] M. A. Soto and L. Thévenaz, "Modeling and evaluating the performance of Brillouin distributed optical fiber sensors," *Opt. Exp.*, vol. 21, no. 25, pp. 31347–31366, 2013.
[2] M. Galal, S. Sebastian, Z. Yang, L. Zhang, S. Zaslawski, and L. Thévenaz, "On the measurement accuracy of coherent Rayleigh-based distributed sensors," *Opt. Exp.*, vol. 29, no. 26, pp. 42538–42552, 2021.
[3] Z. N. Wang, J. J. Zeng, J. Li, M. Q. Fan, H. Wu, F. Peng, L. Zhang, Y. Zhou, and Y. J. Rao, "Ultra-long phase-sensitive OTDR with hybrid distributed amplification," *Opt. Lett.*, vol. 39, no. 20, pp. 5866–5869, Oct. 2014.
[4] F. Rodríguez-Barrios, S. Martín-López, A. Carrasco-Sanz, P. Corredera, J. D. Ania-Castañón, L. Thévenaz, and M. González-Herráez, "Distributed Brillouin fiber sensor assisted by first-order Raman amplification," *J. Lightw. Technol.*, vol. 28, no. 15, pp. 2162–2172, Aug. 1, 2010.
[5] J. Urricelqui, M. Sagues, and A. Loayssa, "Brillouin optical time-domain analysis sensor assisted by Brillouin distributed amplification of pump pulses," *Opt. Exp.*, vol. 23, no. 23, pp. 30448–30458, 2015.
[6] A. Beisenova, A. Issatayeva, S. Korganbayev, C. Molardi, W. Blanc, and D. Tosi, "Simultaneous distributed sensing on multiple MgO-doped high scattering fibers by means of scattering-level multiplexing," *J. Lightw. Technol.*, vol. 37, no. 13, pp. 3413–3421, Jul. 1, 2019.
[7] S. Loranger, M. Gagné, V. Lambin-Iezzi, and R. Kashyap, "Rayleigh scatter based order of magnitude increase in distributed temperature and strain sensing by simple UV exposure of optical fibre," *Sci. Rep.*, vol. 5, p. 11177, Jun. 2015.
[8] F. Monet, S. Loranger, V. Lambin-Lezzi, A. Drouin, S. Kadoury, and R. Kashyap, "The ROGUE: A novel, noise-generated random grating," *Opt. Exp.*, vol. 27, no. 10, pp. 13895–13909, 2019.
[9] P. Lu, S. J. Mihailov, D. Coulas, H. Ding, and X. Bao, "Low-loss random fiber gratings made with an fs-IR laser for distributed fiber sensing," *J. Lightw. Technol.*, vol. 37, no. 18, pp. 4697–4702, Sep. 15, 2019.
[10] L. Thévenaz, "Next generation of optical fibre sensors: New concepts and perspectives," in *Proc. 23rd Int. Conf. Opt. Fibre Sensors*, vol. 9157, Jun. 2014, p. 9157AN.
[11] M. Gagné, S. Loranger, J. Lapointe, and R. Kashyap, "Fabrication of high quality, ultra-long fiber Bragg gratings: Up to 2 million periods in phase," *Opt. Exp.*, vol. 22, no. 1, pp. 387–398, 2014.
[12] P. S. Westbrook, K. S. Feder, R. M. Ortiz, T. Kremp, E. M. Monberg, H. Wu, D. A. Simoff, and S. Shenk, "Kilometer length, low loss enhanced back scattering fiber for distributed sensing," in *Proc. 25th Opt. Fiber Sensors Conf. (OFS)*, Apr. 2017, pp. 1–5.
[13] P. S. Westbrook, T. Kremp, K. S. Feder, W. Ko, E. M. Monberg, H. Wu, D. A. Simoff, and R. M. Ortiz, "Improving distributed sensing with continuous gratings in single and multi-core fibers," in *Proc. Opt. Fiber Commun. Conf.*, 2018, pp. 1–3, Paper W1K.1. [Online]. Available: http://www.osapublishing.org/abstract.cfm?URI=OFC-2018-W1K.1
[14] OFS Optics. (2019). *AcoustiSens Optical Sensor Fiber*. [Online]. Available: https://fiber-optic-catalog.ofsoptics.com/documents/pdf/AcoustiSens-web.pdf
[15] L. Zhang, Z. Yang, N. Gorbatov, R. Davidi, M. Galal, L. Thévenaz, and M. Tur, "Distributed and dynamic strain sensing with high spatial resolution and large measurable strain range," *Opt. Lett.*, vol. 45, no. 18, pp. 5020–5023, Sep. 2020.
[16] M. Galal, S. Sebastian, L. Zhang, and L. Thévenaz, "Distributed temperature sensing based on φ-OTDR using back-reflection-enhanced fiber," in *Proc. CLEO, Sci. Innov.*, 2021, Paper STu1A-3.
[17] X. Lu and K. Krebber, "Characterizing detection noise in phase-sensitive optical time domain reflectometry," *Opt. Exp.*, vol. 29, no. 12, pp. 18791–18806, 2021.
[18] S. Wang, Y. Z. Yang, M. A. Soto, and L. Thévenaz, "Study on the signal-to-noise ratio of Brillouin optical-time domain analyzers," *Opt. Exp.*, vol. 28, no. 14, pp. 19864–19876, Jun. 2020.
[19] M. Alem, M. A. Soto, and L. Thévenaz, "Analytical model and experimental verification of the critical power for modulation instability in optical fibers," *Opt. Exp.*, vol. 23, no. 23, pp. 29514–29532, 2015.
[20] L. Zhang, L. D. Costa, Z. Yang, M. A. Soto, M. Gonzalez-Herraez, and L. Thevenaz, "Analysis and reduction of large errors in Rayleigh-based distributed sensor," *J. Lightw. Technol.*, vol. 37, no. 18, pp. 4710–4719, Sep. 15, 2019.
[21] M. Galal, S. Sebastian, Z. Yang, and L. Thévenaz, "Determination of the measurement accuracy of a phase-sensitive OTDR," in *Proc. OSA Opt. Sensors Sens. Congr.*, 2021, Paper SM5A.5.

MALAK GALAL received the B.Sc. degree in information engineering and technology majoring in electronics engineering from German University in Cairo (GUC), Egypt, in 2017. In 2018, she joined the Group for Fiber Optics, Ecole Polytechnique Fédérale de Lausanne (EPFL), Switzerland, as a Doctoral Research Assistant. Her research interests include distributed optical fiber sensing in different types of fibers, such as standard single-mode, reflection-enhanced, and hollow core fibers. She is a Student Member of Optica.

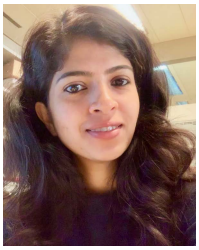

SUNEETHA SEBASTIAN received the Ph.D. degree in photonics from the International School of Photonics, Cochin University of Science and Technology (CUSAT), India, in 2016. She was a National-Post Doctoral Fellow funded by the Department of Science and Technology (DST), Government of India, and the Department of Instrumentation and Applied Physics, Indian Institute of Science, Bengaluru, India, from 2016 to 2017. From 2017 to 2020, she worked at the Indian Institute of Science as a DST-INSPIRE Faculty, awarded by the Government of India. From 2019 to 2020, she worked as a Visiting Faculty/Researcher at the Group for Fiber Optics, Institute of Electrical Engineering, Ecole Polytechnique Fédérale de Lausanne (EPFL), Switzerland. She is currently working as a Postdoctoral Researcher at the Group for Fiber Optics, EPFL. Her main research interests include optical fiber sensing using fiber Bragg grating sensors and distributed optical fiber sensors. She is a member of Optica.

LUC THÉVENAZ (Fellow, IEEE) received the M.Sc. and Ph.D. degrees in physics from the University of Geneva, Geneva, Switzerland. In 1988, he joined the Ecole Polytechnique Fédérale de Lausanne (EPFL), Switzerland, where he currently leads a research group (Group for Fiber Optics) involved in photonics, namely fiber optics and optical sensing. He achieved with his collaborators the first experimental demonstration of optically controlled slow and fast light in optical fibers, realized at ambient temperature and operating at any wavelength since based on stimulated Brillouin scattering. He also contributed to the development of Brillouin distributed fiber sensing by proposing innovative concepts pushing beyond barriers. During his career, he stayed at Stanford University, the Korea Advanced Institute of Science and Technology, Tel Aviv University, The University of Sydney, and the Polytechnic University of Valencia. In 2000, he cofounded the company Omnisens that is developing and commercializing advanced photonic instrumentation based on distributed fiber sensing. His research interests include Brillouin-scattering fiber sensors, slow and fast light, nonlinear fiber optics, and laser applications in gases. He is a fellow of Optica. He is the Chair of the International Conference on Optical Fiber Sensors and the Co-Executive Editor-in-Chief of *Light: Science & Applications* (Nature).